INSTITUTE OF PHYSICS PUBLISHING SUPERCONDUCTOR SCIENCE AND TECHNOLOGY

Supercond. Sci. Technol. **14** (2001) 433–443 www.iop.org/Journals/su PII: S0953-2048(01)22405-1

Design, fabrication and performance of a 1.29 T Bi-2223 magnet

A B Sneary[1], **C M Friend**[2] **and D P Hampshire**[1]

[1] University of Durham, Department of Physics, South Road, Durham DH1 3LE, UK
[2] BICC General Superconductors, Oak Road, Wrexham LL13 9XP, UK

Received 16 February 2001

Abstract

The design and fabrication procedure of a laboratory-scale Bi-2223 tape superconducting magnet with a bore of 40 mm and a maximum field of 1.29 T at 4.2 K is presented. The magnet comprises six resin impregnated double-wound pancakes of bore diameter 40 mm fabricated via the react-and-wind route. Critical current density (J_c) measurements have been made as a function of magnetic field, angle and strain at 4.2 K and 77 K on short samples. In zero field, the critical current density for the superconducting cross-sectional area of the tape was 8.3×10^4 A cm^{-2} (4.2 K) and 1.18×10^4 A cm^{-2} (77 K). The electric field–current density characteristics of all the components of the coils when individually energized or with the whole magnet energized have been measured. Comparison between short sample measurements and performance of the magnet show that minimal additional damage occurred beyond the ∼20% that was produced by the bending strain during the wind-and-react fabrication procedure and the ∼10% variation of the long length J_c of the tape. Sufficient detail is provided for the non-specialist to assess both the use of potential brittle superconducting tapes for magnet technology and to construct a laboratory-scale magnet.

1. Introduction

Since the discovery of Bi-based high-temperature superconducting ceramics [1, 2], an enormous effort has gone into improving the critical current density (J_c) of these materials. In short samples, J_c of 6.9×10^4 A cm^{-2} [3] and 7.3×10^4 A cm^{-2} [4] has been achieved in zero-field at 77 K. High-field applications rely on the use of high-performance tapes of kilometre lengths. In the Bi-2223 system, this level of performance is now being realized with J_c of 1.2×10^4 A cm^{-2} reported over 1260 m [5], 1.8×10^4 A cm^{-2} over 250 m [6] and over 2×10^4 A cm^{-2} achieved in 1200 m [7], 1000 m [8] and 400 m [9] lengths at 77 K in self-fields. It is expected that J_c will increase yet further, perhaps by an order of magnitude [10], as our understanding of tape processing improves.

The high current-carrying capacity of Bi-2223 up to 30 K [7, 11, 12] enables the production of compact cryogen-free magnet systems. Cryogen-free systems are attractive because: (i) easy operation is facilitated since no cryogen is required; (ii) cooling efficiency at 20 K is approximately five times higher than at 4 K making refrigeration more economical; (iii) thermal stability and fast magnet sweep rates are possible because the specific heat of the tapes is about two orders of magnitude higher at 20 K than at 4 K. Cryogen-free Bi-2223 systems have been fabricated using stacked pancake coils producing fields of 7.25 T [13] and 7 T [14] at around 20 K. The high upper critical field of Bi-2223 also facilitates the production of high-field inserts. A record field of 24 T at 4.2 K [7] was achieved from a Bi-2223 insert in a 22.54 T background field, the same magnet producing 2.3 T at 4.2 K in a self-field. A magnet producing 3.2 T in a self-field and 1 T at 4.2 K in a background field of 20 T has been fabricated [5]. Inevitably the enormous effort producing large-scale Bi-2223 magnets and inserts has led to the proprietary use of materials and commercial knowledge.

Increasing opportunities for fabricating laboratory-scale magnets in the 1–5 T range operating at temperatures below 30 K will follow the improvements in J_c of Bi-2223 tapes. Laboratory-scale magnets have been produced using both the 'react-and-wind' (R + W) and 'wind-and-react' (W + R) processes. Using R + W, 1 T has been generated [15] from eight R + W double-wound pancakes at 4.2 K. At 20 K, 1.1 T was achieved from 17 R + W double-wound pancakes [16]. Using W + R, a Bi-2223 coil with a 15 mm bore generated a field of 1.34 T at 4.2 K [17] and Bi-2212 inserts have produced 2.6 T in a self-field and 1.08 T in a background of 20 T at

Table 1. The main parameters and dimensions of the Bi-2223 tapes.

	Tape 1	Tape 2
Material	Bi-2223	Bi-2223
Sheath	Silver alloy Ni/Mg	Silver alloy Ni/Mg
Thickness (mm)	0.33	0.29
Width (mm)	3.3	3.5
Number of filaments	37	37
Fill factor (%)	28	28
Length of tape (m)	120	70
I_c of sections along tape length at 77 K, zero magnetic field (A)	35–38	33–35

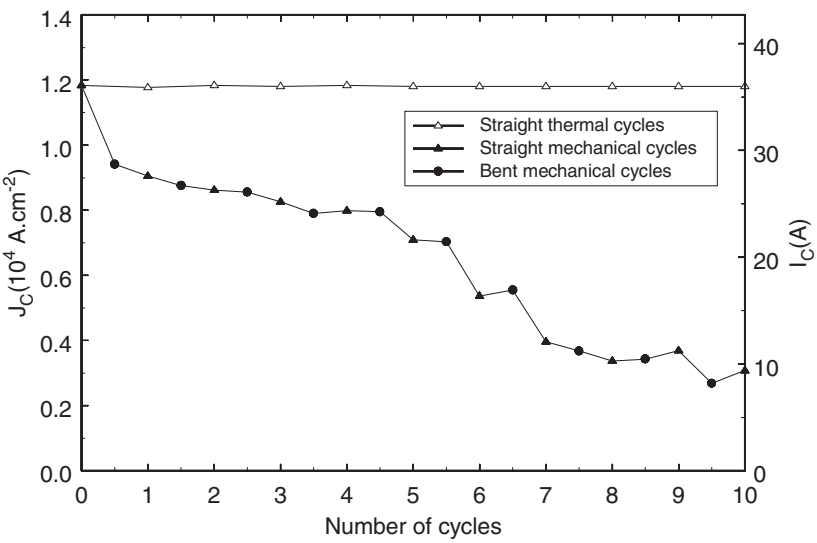

Figure 1. The critical current density (J_c) of thermally and mechanically cycled 100 mm samples of Bi-2223 tape at 77 K. The open symbols (△) are for thermally cycling alone. The closed symbols are for a tape that is bent (●) and J_c measured, and then straightened (▲) and remeasured for 10 cycles.

4.2 K [18]. This paper includes an outline of the fabrication of a laboratory-scale magnet that was produced without the use of specialist equipment (e.g. coil winding machines).

In section 2, J_c data for short samples of Bi-2223 tape are presented and used to assess the effects of magnetic field, strain and anisotropy. In section 3, the design and fabrication procedure for the Bi-2223 magnet system consisting of six double wound pancakes is presented. Since the design parameters of any laboratory-scale magnet are specific to the application including magnitude of field, field homogeneity, reinforcement of the structure and bore size, alternative available fabrication options are also discussed. In section 4, J_c data for the magnet and all constituent pancakes at 4.2 K and 77 K are presented. Axial field profiles of the magnet, measured using a Hall probe, are compared with calculations. The electric field–current density (E–J) characteristics of all pancakes were measured both with each coil (i.e. double pancake) individually energized and with the magnet energized to assess the reliability of the fabrication route. In section 5, the performance of the coils and pancakes is compared with calculations which together demonstrate that the magnet presented produced a field close to short-sample performance. The discussion in section 6 considers the data presented and suggests a series of experiments required to efficiently assess the suitability of a particular tape for a particular application. In this paper, sufficient detail is included so that the non-specialist can assess both the performance of available brittle superconducting tapes for magnet technology and then design and fabricate a R + W laboratory-scale magnet using pancake coils with equipment available in any well-founded laboratory.

2. Measurements on a short sample of a BiSCCO tape

Once the basic design parameters of magnet bore size and dimensional restrictions are determined (cf section 4), the field strength of modern magnets is almost entirely determined by the performance of the superconducting wire or tape [19]. In our magnet, system restrictions include a minimum bore diameter of 40 mm, maximum outer diameter of 82 mm and use of the R+W conductor. In this section, short samples of the BiSCCO tape used to fabricate the magnet are characterized. The tapes used were 37 filament Bi-2223 alloy sheathed tape fabricated via the powder-in-tube (PIT) route with J_c of 8.3×10^4 A cm^{-2} (4.2 K, 0 T) across the superconducting cross section. The parameters of the two constituent tapes are presented in table 1. In Bi-2223, it is known that J_c is strongly dependent on the magnitude of the field [7, 11, 12], angle of the applied field [20–26] and strain [27–30].

Figure 1 shows the effects of thermal and mechanical cycling on the critical current density of tape 1 at 77 K and zero field using 100 mm samples. The straight sample J_c was

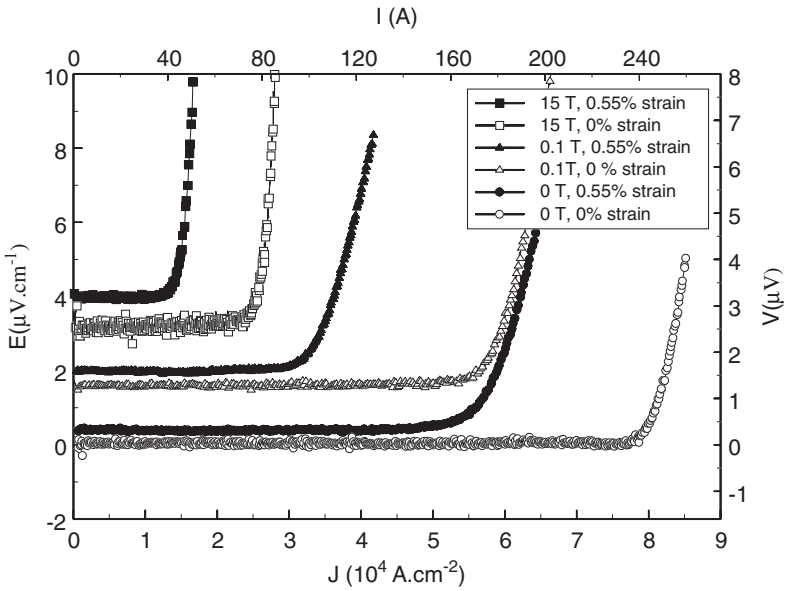

Figure 2. E–J traces for short samples of Bi-2223 tapes at 0% and 0.55% strain at 4.2 K in fields up to 15 T.

measured as 1.18×10^4 A cm^{-2} (77 K, 0 T) using a criterion of 1.5 μV cm^{-1}. After 10 thermal cycles no degradation was observed in J_c within the experimental limits. In a second experiment, the sample was mechanically cycled by bending it around a 44 mm diameter (the diameter of the inner turn of the magnet) and then re-straightening. J_c was measured in each configuration (1 thermal cycle includes two J_c measurements) during 10 mechanical cycles. The first mechanical cycle produced a permanent decrease in J_c of ∼20%. Eventually the J_c degraded by ∼75% from the straight sample performance.

The field dependence of J_c was measured using 30 mm samples of tape 1 at 4.2 K in fields up to 15 T. Measurements were taken on a straight sample (0% strain) and a sample bent on a 44 mm diameter (0.55% strain). Strain values quoted in this paper were calculated using $\varepsilon = t/D$, where t is the thickness of the superconductor (0.24 mm) and D is the bending diameter. J_c of the tape was 8.3×10^4 A cm^{-2} (4.2 K, 0 T, $\varepsilon = 0\%$) and 5.82×10^4 A cm^{-2} (4.2 K, 0 T, $\varepsilon = 0.55\%$). Data were taken with the field applied in two and three orthogonal directions with respect to the surface of the tape for the 0.55 and 0% strained samples, respectively. Typical E–J characteristics are presented in figure 2 for the field applied parallel to the tape surface (B parallel to a–b planes) in fields up to 15 T. At all fields the strain degrades J_c. However, all traces produce flat baselines to within the noise (200 nV peak-to-peak) suggesting that undamaged filaments of zero resistance exist within the strained sample. In figure 3, the J_c for tape 1 at 4.2 K in fields up to 15 T with field applied parallel and perpendicular to the tape surface at 0 and 0.55% strains were determined using a criterion of 1.5 μV cm^{-1}.

Once the short sample behaviour of the conductor has been measured the optimum performance of the magnet can be calculated prior to magnet fabrication assuming that short sample performance is achieved in long lengths. These calculations are addressed in section 4.

3. Magnet fabrication

3.1. Magnet windings

The choice of conductor determines whether the R + W, W + R [6, 17, 31, 32] or wind, react and tighten (WRAT) [18, 33] methods are most suitable. W + R routes have facilitated the production of pancake coils with radii ∼5 mm showing no degradation in J_c [31]. The degradation in tape performance from the more simple R + W technique due to strain on the conductor that was used in this work should be weighed against the high melting point insulation and accurate reaction conditions for the coils required in the W + R technique. We calculate that a ∼20% increase in maximum field would have occurred had a strain-free W + R technique been used.

PIT tape was used in this magnet. There is a continuing effort to improve processing of PIT tapes, in which precursor powders are packed into silver alloy tubes, drawn and pressed into a tape and processed in complex thermomechanical heat-treatment schedules [5, 34–41]. Other long-length tapes include dip coating [18, 33, 42] and electrophoretic deposition [43].

The tape was wound onto Tufnol bobbins of thickness 2 mm and inner diameter 40 mm. Tufnol was chosen primarily because of its electrically insulating properties and ease of use but also due to its adequate fracture stress and similar thermal contraction to epoxy. Copper and other metallic based materials have been used with the advantages of higher thermal conductivity and high strength which can be important in large magnets [7, 15, 16]. Ceramic formers are used in W + R magnets due to their refractory properties [6, 32].

The bobbins were covered by a single layer of glass fibre tape and placed on a polytrifluorochloroethylene (PTFE) mount as shown in figure 4(a). Each coil contained two oppositely wound pancakes joined together at the bottom turn using Bi-2223 strips. The tape was wound into anchor points in the Tufnol bobbin and soldered across the short orthogonal tapes that provided electrical connections between

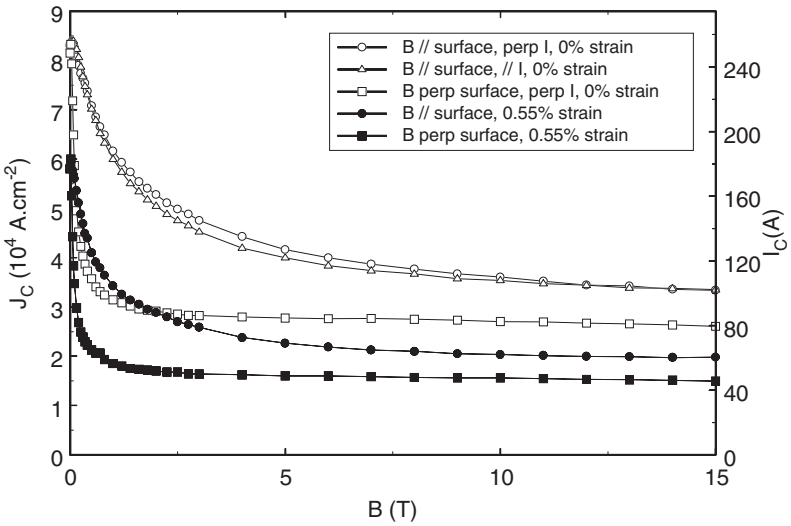

Figure 3. The critical current density as a function of magnetic field for a short sample of Bi-2223 tape 1 at 0% and 0.55% strain with field aligned parallel and perpendicular to the tape surface. All data taken at 4.2 K.

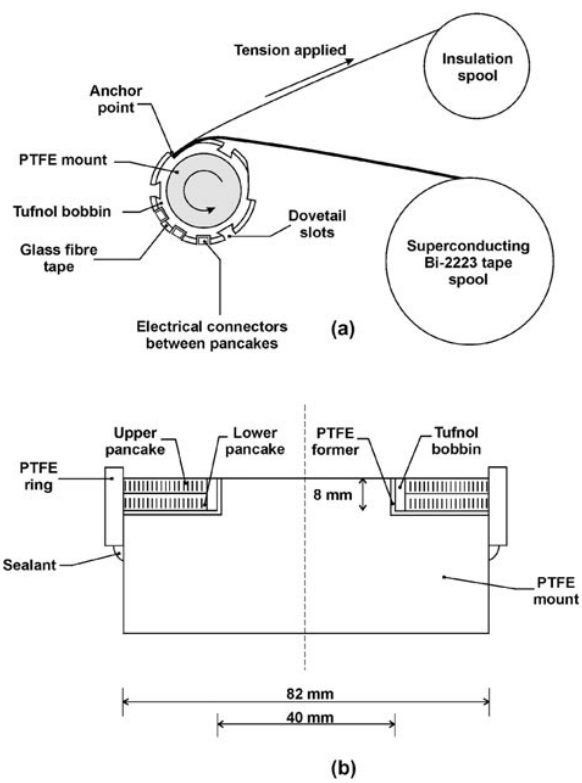

Figure 4. (a) The experimental arrangement for winding the tape and insulation onto the Tufnol bobbin. (b) The PTFE components used during the vacuum resin impregnation.

the two pancakes. The superconducting tape was co-wound with non-adhesive polyimide (Kapton) tape of thickness $\sim$60 μm to provide turn-to-turn insulation. The insulation was tensioned during winding to maximize the radial packing factor although the superconductor was not tensioned in order to minimize damage. Polyimide is usually selected since it is an insulating material available in thin tape form ($\sim$60 μm) which has a high (short period) melting point of 310 °C and reasonable strength (for winding under tension) [7, 14, 16, 44]. Alternatives include Mylar, braid or a varnish coating for R + W [45, 46] and alumina based slurries for W + R coils [6, 17, 31, 32, 47, 48]. One polyimide sheet was inserted to provide pancake–pancake insulation. After the first pancake was wound, the superconducting spool was turned round and repositioned so that the strain was minimized (i.e. the tape was not straightened) while winding the second pancake. Finally a Bi-2223 current lead was soldered to the outer turn of each pancake and copper voltage taps were soldered onto the inner and outer turns of each pancake to facilitate diagnostic measurements on all sections of the coil. Six double-wound pancake coils were fabricated. The parameters of each coil are presented in table 2.

The windings of a superconducting magnet system must be completely impregnated by insulating material which ensures that the turns do not move when the magnet is energized. Such movement can quench the magnet and damage the brittle conductor. Ideally the impregnant should have a high fracture stress at operating temperature, have similar thermal contraction properties to the superconductor and be adhesive to the turns. Standard choices are wax (often preferred for small coils which are seldom thermally cycled) and resin (Araldite or Stycast) [46, 49]. The thermal and mechanical properties vary for different resin systems but for small magnets the ease of use and pot-life are primary considerations [50–54]. To key the resin to the bobbins, dove tail slots were incorporated into the bobbin (cf figure 4). For the magnet presented here, a Ciba-Geigy resin system CY1300 (resin), HY906 (hardener) and DY073 (accelerator) mixed in the ratio 100:80:2 by weight respectively was used. During impregnation the coils and resin were held in the PTFE parts which constitute the mould shown in figure 4(b). PTFE was used because of its non-stick properties. The resin was degassed for 12 h at 50 °C. The coil was then impregnated with resin under vacuum at 50 °C. On completion of impregnation, the system was let up to atmospheric pressure to drive the resin into the turns. The temperature was then increased to 80 °C and held for 16 h before curing at 120 °C for 8 h. A minimum volume of resin was used to avoid any resin-rich areas that are

Table 2. The main parameters of the constituent coils of the Bi-2223 magnet.

	Coil 1 (top)			Coil 2			Coil 3		
Pancake	lower	upper	whole	lower	upper	whole	lower	upper	whole
Tape	1	1	—	1	1	—	1	2	—
Height (mm)	—	—	8.5	—	—	8.0	—	—	8.5
Number of turns	43	41	84	43	43	86	43	50	93
Length of tape (m)	8.51	8.11	16.62	8.51	8.51	17.02	8.51	9.90	18.41
Packing factor (%)	—	—	64.0	—	—	69.6	—	—	65.8
	Coil 4			Coil 5			Coil 6 (bottom)		
Pancake	lower	upper	whole	lower	upper	whole	lower	upper	whole
Tape	2	2	—	1	1	—	1	1	—
Height (mm)	—	—	8.5	—	—	8.5	—	—	9.5
Number of turns	50	50	100	43	43	86	43	39	82
Length of tape (m)	9.90	9.90	17.80	8.51	8.51	17.02	8.51	7.72	16.23
Packing factor (%)	—	—	66.0	—	—	65.5	—	—	55.9

Table 3. Mechanical properties of the constituent materials of the Bi-2223 magnet.

	Epoxy resin [46]	Tufnol (Carp)[a]	Polyimide [70]	Bi-2223/Ag [59]
Thermal contraction at 4.2 K (%)	1.1	0.57	0.9	0.25
Yield/fracture stress (MPa)	140	105[b]	155	—

[a] Manufacturer's specification.
[b] Room temperature.

particularly liable to crack during thermal cycling. The coil was removed from the PTFE mould after curing.

In a solenoid the Lorentz forces act to compress the magnet axially and explode it radially. These forces act to deform the constituent materials which will modify J_c and can, if excessive, lead to catastrophic failure. Formulae for calculating stresses in magnets are well established [46]. If the fracture stress of any of the constituent materials is exceeded [55], reinforcement should be included such as co-winding thin stainless-steel tapes with the superconductor [7, 14, 17, 44, 56, 57], reinforcing sections of the magnet [58] or having a support structure around the outside of the magnet [46, 58]. Fibre reinforced plastic (FRP) sheets are frequently used to insulate and reinforce the magnet in the axial direction [6, 7, 44]. Estimates of the maximum stress produced in our magnet are around 150 kPa, which is much less than typical fracture/yield stresses of the constituent materials (listed in table 3). Typically no additional reinforcement is required for properly impregnated laboratory-scale magnets.

Coils were stacked and glued together to form the magnet using the Ciba-Geigy room-temperature curing system CY1300 (resin) and HY1300 (hardener) mixed in the ratio 3:1 by weight. Joints between the coils were made by soft soldering Bi-2223 tape connections. Although sophisticated jointing techniques have been developed, this is rarely necessary in small magnet systems [32, 49]. The magnet was supported between two non-magnetic stainless-steel plates (brass is equally good) using four support rods. A top plate was connected above the top support plate with 24 voltage terminals, to allow the voltage across any pancake to be measured. Current access to all coils was also provided via seven current terminals on the top plate electrically connected to the coils with Bi-2223 tape which allowed any coil to be individually energized as well as the entire magnet. The dimensions of the Bi-2223 magnet are presented in table 4 and a photo shown in figure 5.

Table 4. Dimensions and characteristic properties of the Bi-2223 magnet.

Bore (mm)	40
Magnet winding I/D (mm)	44
Magnet winding O/D (mm)	82
Magnet height (mm)	57.5
Number of double pancakes	6
Length of Bi-2223 tape (m)	103.1
Magnet packing factor (%)	58
Central bore field constant (mT A^{-1})	8.18
Maximum field constant (mT A^{-1})	8.85

3.2. External components

Copper current leads were used from the top of the cryostat to the magnet current terminals. The large heat leak to the system due to the copper leads was considered acceptable during the eight day testing period. Optimized permanent current leads are typically fabricated from tubes of brass with a current density × length product of 1.5×10^6 A m^{-1} for operating at 4.2 K and 6×10^6 A m^{-1} at 77 K [46, 59, 60].

Quench protection is an essential component in large superconducting magnets because of the large potential energy stored when energized (∼1–10 MJ). Critical parameters include the maximum temperature (θ_{MAX}) and the maximum

Figure 5. Photo of Bi-2223 magnet.

voltage (V_{MAX}) together with the characteristic decay time for the current decay following a quench. A maximum temperature of 100 K is normally considered safe enough to ensure that the local expansion in the region of the (hot) quench does not damage the windings, although 500 K can be tolerated in some systems without mechanical damage or the insulation or resin melting. The breakdown voltage for polyimide is 120 kV mm^{-1} and for polymer resins is typically tens of kV mm^{-1}. The basic approach to protecting a large magnet if θ_{MAX} or V_{MAX} are too large is to subdivide the magnet. Choices include active and passive systems either within or outside the cryostat [46, 61]. Basic calculations suggest that no sub-division (and protection) is required if the magnet, as is the case here, consists of less than 2 km of wire or tape [19].

The inclusion of iron pole pieces [62, 63] or copper coils [64] has been shown to reduce the magnitude of the radial field component in the outer coils and therefore increase the field produced by the magnet. This approach is only applicable for low field systems where the iron does not saturate. It has been suggested that the maximum radial component may be reduced by ∼40% [63]. Calculations suggest that such a reduction may have produced up to ∼15% increase in maximum field.

4. Performance of coils and magnet

After each coil was fabricated, it was tested at 77 K to identify any damage or electrical problems. The I_c values obtained after initial cool-down using the 1.5 μV cm^{-1} criterion are presented in table 5. There is relatively large variation from coil to coil, primarily because the number of turns and geometry of the coils are not the same. In addition, after the first pancake of a coil is tested, subsequent measurements on the second pancake and joints are affected by a remnant field and possibly because the coil had not cooled back to 77 K. However, since these 'quality control' experiments showed that there was no evidence of significant damage, all coils were stacked to form the magnet.

E–J measurements were taken for each coil when individually energized (to identify any damaged pancakes) at 4.2 K and 77 K (not shown), with the whole magnet energized and with the magnet energized in a background field at 4.2 K and 77 K. The background field of 296 mT at 4.2 K and 40 mT at 77 K was provided using a large bore Bi-2223 system which has been previously reported [65]. Comparing the I_c values for any pairs of pancakes in a given coil when individually energized, one finds that for tape 1 the variation in I_c is ∼7% and for tape 2 it is ∼5%. These variations are consistent with long-length variations in I_c in the original tape of up to ∼10%.

The E–J characteristics obtained from coil 1 individually energized at 4.2 K and its component pancakes are presented in figure 6 and for coil 5 with the whole magnet energized at 4.2 in figure 7. In both cases the baselines are flat (consistent with the short sample data in figure 2), the superconducting joint resistance remains low for $I < I_c$ and the E–J characteristics of the whole coil is the sum of the pancakes and connecting joint. When the whole magnet is energized, the top and bottom coils exhibit the lowest I_c at both 4.2 (90 and 92 A) and 77 K (12.6 and 11.7 A), consistent with other work in the literature [64–66]. Typical joint resistances between pancakes are below 2 $\mu\Omega$ at 100 A at 4.2 K. The I_c of the magnet in a self-field was measured to be 104 A at 4.2 K and 12.8 A at 77 K.

The axial field profile along the central bore axis was measured using a Hall probe at room temperature with the magnet energized at 1.0 A. The field profile within the magnet was calculated to high precision by taking into account the precise number of turns on each pancake, the packing factor and the position and geometry of each pancake [67]. In figure 8, the excellent agreement found between the calculated and measured profiles provides evidence that there are no short-circuited turns within the magnet. The measured maximum field constants of 8.18 mT A^{-1} at 4.2 K and 8.20 mT A^{-1} at room temperature agree to better than 1% with the calculated value of 8.11 mT A^{-1}. The axial field is homogeneous to ∼1.5% over 1 cm about the centre.

The optimum shape for small magnets is a (well documented) compromise between the magnitude of the field produced, the homogeneity of the magnetic field profile and the length of conductor [46]. A coil that has a minimum weight of wire for a given field will produce a homogeneity of ∼1 part

Table 5. I_c test results of all constituent pancakes and coils of the Bi-2223 magnet at 4.2 and 77 K. At 77 K, each coil was individually energized and tested before stacking whereas at 4.2 K the equivalent measurement was taken after stacking. The electric field criterion used for I_c was 1.5 μV cm^{-1}.

	Coil 1 (top)			Coil 2			Coil 3		
Pancake	lower	upper	whole	lower	upper	whole	lower	upper	whole
4.2 K									
I_c for individually energized coils (A)	115	123	124	120	127	127	115	103	111
n-index	14.7	20.0	—	16.7	16.7	—	16.1	14.9	—
I_c for magnet energized (A)	99	90	95	112	110	111	—	110	114
I_c for whole magnet energized in 296 mT background field (A)	96	88	95	109	109	109	119	106	113
77 K									
I_c for individually energized coils (A)	18.3	14.9	15.8	20.1	16.4	17.2	19.1	13.7	14.8
n-index	9.7	9.0	8.6	10.5	10.2	9.2	10.5	10.3	9.8
I_c for whole magnet energized (A)	13.5	12.6	13.3	16.0	15.2	15.8	17.9	15.7	16.5
I_c for whole magnet energized in 296 mT background field (A)	12.7	12.2	12.6	15.3	14.6	14.8	16.7	14.9	15.4

	Coil 4			Coil 5			Coil 6 (bottom)		
Pancake	lower	upper	whole	lower	upper	whole	lower	upper	whole
4.2 K									
I_c for individually energized coils (A)	104	108	105	130	128	130	123	120	—
n-index	15.2	17.3	—	16.3	15.9	—	15.1	15.3	—
I_c for magnet energized (A)	107	117	110	107	115	111	92	100	94
I_c for whole magnet energized in 296 mT background field (A)	107	117	112	108	115	109	88	97	95
77 K									
I_c for individually energized coils (A)	17.7	14.7	15.3	19.2	16.0	16.9	17.5	15.3	16.0
n-index	11.5	11.3	10.9	10.3	10.3	9.6	9.8	9.1	9.1
I_c for whole magnet energized (A)	15.3	17.6	15.8	14.7	16.1	15.9	11.7	14.0	12.5
I_c for magnet energized in 40 mT background field (A)	14.6	16.3	15.0	14.0	15.5	14.7	11.3	13.0	12.1

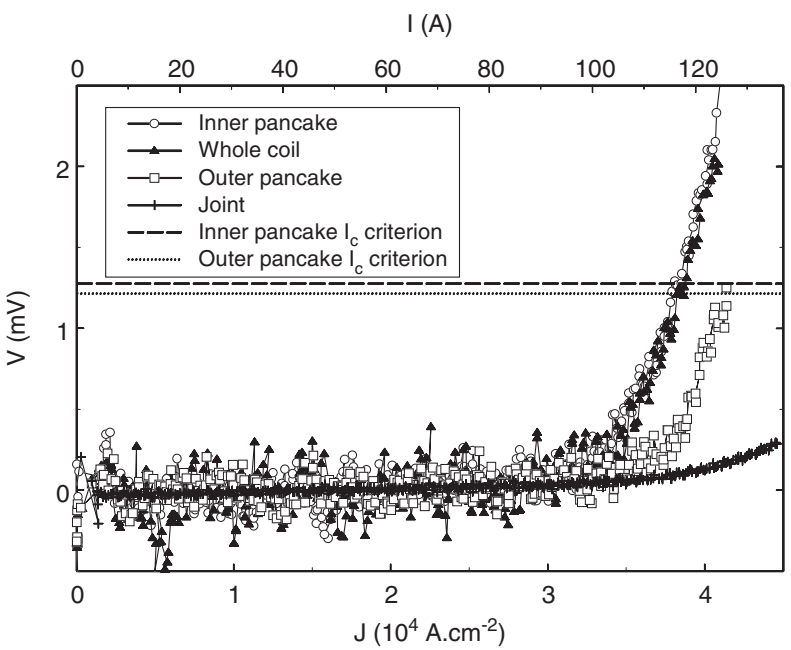

Figure 6. Electric field–current density characteristics of the components of coil 1 with the coil individually energized at 4.2 K.

in 10^3 over a 1 cm diameter sphere volume. For higher homogeneity up to 1 part in 10^5, notch, compensation or shim coils may be added [19, 68]. The maximum magnet constant for our magnet is calculated as 8.85 mT A^{-1}, positioned on the inner winding at 2 mm above the centre. This maximum is offset from the centre due to the asymmetry of the number of turns. The maximum current passed through the magnet in a self-field was 146 A at 4.2 K, limited by a 10 V power

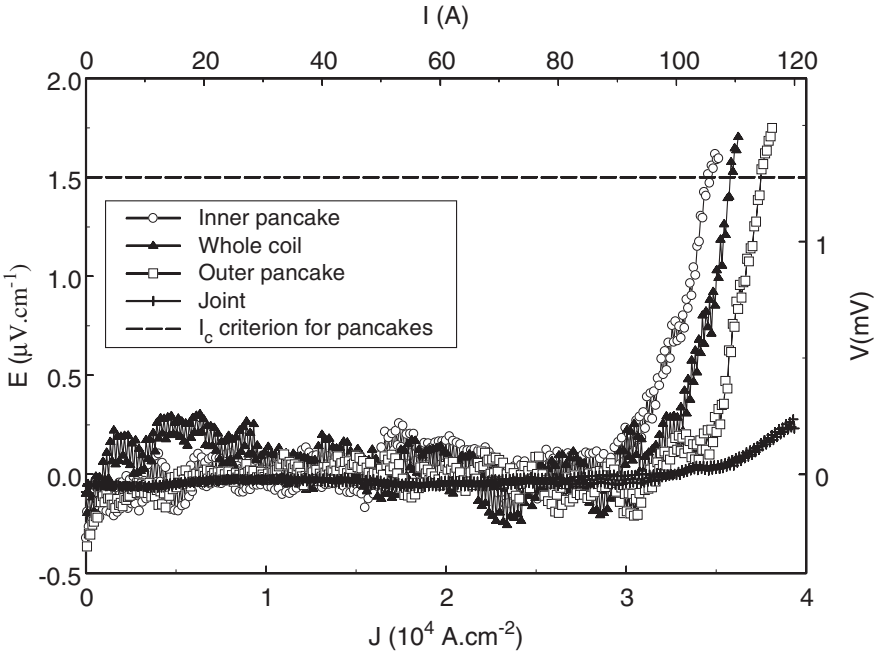

Figure 7. Electric field–current density characteristics of the components of coil 5 with the whole magnet energized at 4.2 K.

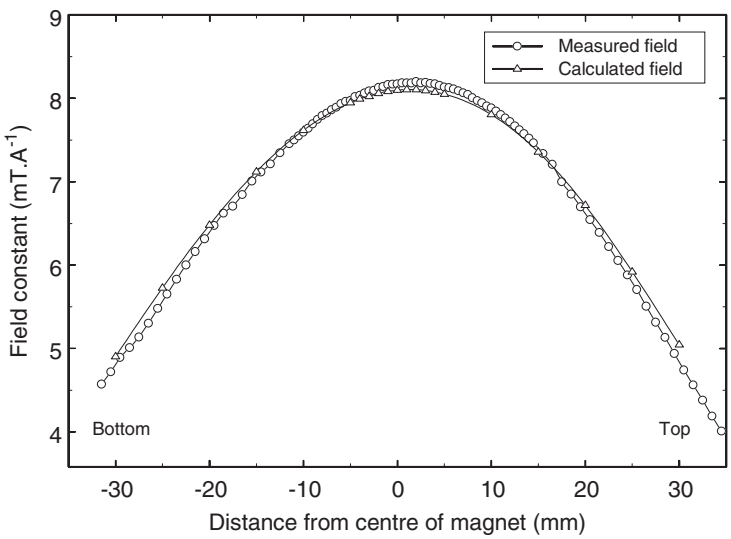

Figure 8. Comparison between measured and calculated axial field profiles within the Bi-2223 magnet.

supply, corresponding to a maximum bore field of 1.19 T and a maximum magnet field on the turns of 1.29 T. In a background field at 4.2 K the maximum measured bore field was 1.470 T (including 296 mT contribution from the large bore magnet).

5. Calculations of magnet performance

The I_c of any turn in any pancake is determined by the local angle and magnitude of the magnetic field and the local strain state. The magnitude and direction of field throughout the magnet has been calculated using standard formulae. The field profile of the magnet was generated using the precise dimensions of each coil. The geometry and number of turns of coil 2 were used in calculations for the individually energized coils. The strain state was calculated from the bending radius.

It is a very large experimental task to determine the magnetic field, temperature and strain dependence of J_c for a short sample throughout the superconducting phase. To approximate the functional form of J_c over the required range, we have chosen to linearly interpolate the variable magnetic field J_c data in figure 3 obtained at two different orientations of the field and two different strains. Comparison with the literature shows that these interpolations give a reasonable first approximation to the observed Bi-2223 J_c dependence on strain [27–30] and angle [20–26] as discussed in section 6.

The positions of the turns with the lowest I_c (i.e. the performance limiting turn) were identified at $r = 36$ mm (105 A) for the individually energized coils and on the top and bottom pancake at $r = 38$ mm (94 A) for the fully energized magnet. The J_c dependences and corresponding

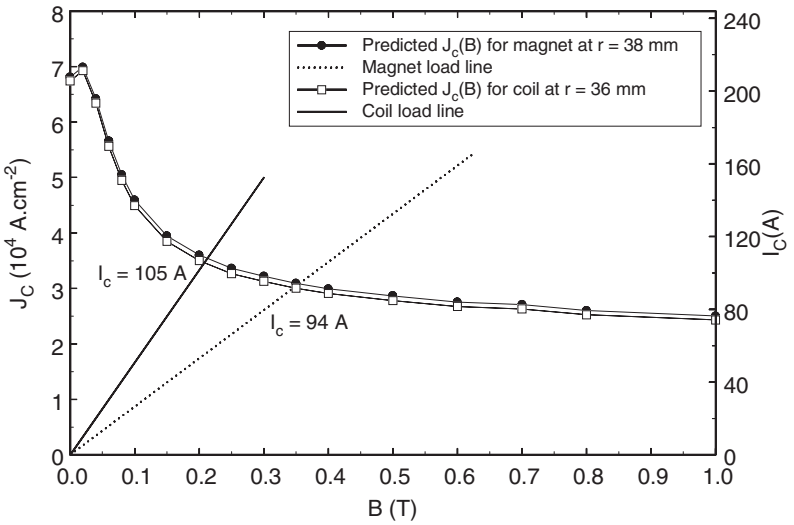

Figure 9. The field dependence of the critical current density calculated for the turn at $r = 36$ mm in an individually energized coil and for the turn at $r = 38$ mm on the outermost pancake with the magnet energized. The associated load lines are also shown.

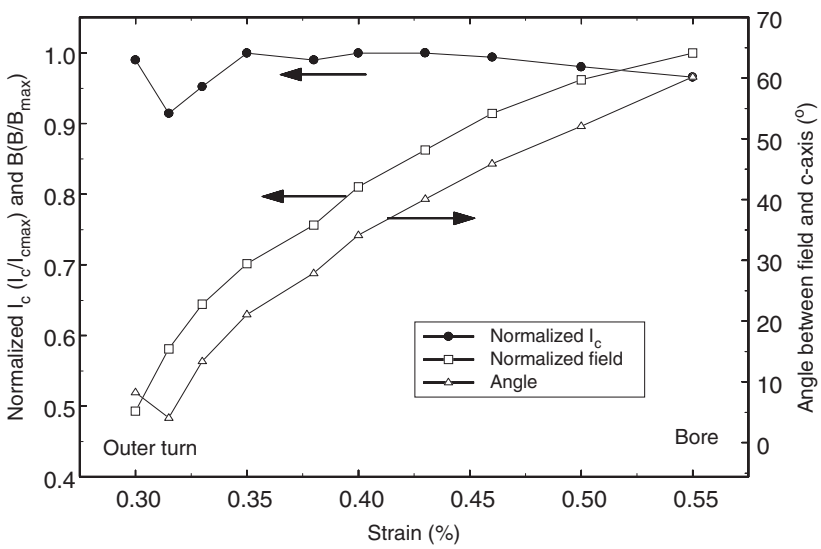

Figure 10. The change in the normalized critical current (•), normalized magnetic field (□) and angle of field (△) from the c-axis as a function of strain for turns across the outermost pancake with the magnet energized. I_c is normalized to the value of the outer turn and the field is normalized to the field experienced by the inner turn.

load lines for the performance limiting turns are presented in figure 9. The change in the normalized current density within the top pancake when the magnet is energized is presented in figure 10 where calculations for J_c were made at 2 mm intervals radially along the pancake. The changes in magnitude and direction of the field experienced by the turns are presented in the same figure. On moving radially outwards from the bore the magnitude of the field decreases by 50%, the strain decreases by 45% and the angle of the field becomes more closely aligned with the c-axis of the tape by 60°. The combined effect of these factors results in only a 10% variation in I_c across the pancake. The calculated I_c of the top pancake is 94 A. Above 94 A, heat will start to be generated locally. An average value of I_c(av) for the pancakes has also been calculated using a length average defined by $I_c(\text{av}) = \sum I_c l / \sum l$ where l is a length of tape with a particular I_c. For an individually energized coil, I_c(av) is 115 A and 101 A across the top coil with the magnet energized. The measured I_c values of 90 and 92 A for the top and bottom pancakes with the magnet energized (cf table 5) are in good agreement with the calculated value of 94 A.

The performance of the magnet has also been calculated assuming a W + R approach. Necessarily, there is no degradation in the tape performance due to strain. In the case of the individually energized coil, the performance limiting turn is positioned at $r = 36$ mm with an I_c value of 133 A. With the magnet energized, the performance limiting turn is positioned at $r = 38$ mm on the outermost pancake with an I_c of 117 A. Hence the maximum field could be increased by ∼20%.

6. Discussion

We estimate the uncertainty in the predicted J_c due to the anisotropy and field interpolation to be less than ∼5% given

that the field at the performance limiting turn is aligned with the c-axis to $\sim 5^\circ$ (cf figure 10). The interpolation to determine the strain dependence of J_c within the magnet is more complex. Our experience measuring the strain dependence of J_c in brittle Bi-2223 tapes is that there is considerable statistical variation in short sample measurements [69], probably because of the variation in porosity of the tapes along their length [10]. It is therefore difficult to obtain variable strain short sample data that are representative of long lengths. Nevertheless, in light of the $\sim$10% variation in I_c over long lengths in the tapes and the $\sim$20% degradation in I_c due to strain intrinsic to the R + W technique, there is very good agreement between the calculations and the final magnet performance. We conclude that a reliable fabrication process has been developed for laboratory-scale magnets which produces minimal additional damage due to handling.

We suggest fabrication of a laboratory-scale magnet as follows; measure J_c of the tape as a function of field with the field applied parallel and orthogonal to the tape surface in the unstrained state and at the strain state equal to that on the bore of the proposed magnet; measure J_c after many thermal cycles to ensure no degradation occurs; calculate the performance of the proposed magnet; if necessary a third interpolation point can be obtained on a short sample as a function of the field at the strain state and orientation of the magnetic field for the turn with the lowest I_c, and the expected performance of the magnet double-checked; construct the coils; test the coils in a self-field at 77 K and replace any damaged ones; finally stack the coils to form the magnet.

7. Conclusions

In this paper, the design and fabrication of a 1.29 T laboratory-sized Bi-2223 magnet operating at 4.2 K has been described. The magnet was fabricated from six resin impregnated double-wound pancakes of inner diameter 40 mm wound via the R+W route using Bi-2223/Ag tape with critical current density 8.3×10^4 A cm^{-2} (4.2 K, 0 T). Design considerations actually used and other possible options in fabricating a similar-sized magnet with different operational requirements or restrictions have been discussed.

The measured performance of the magnet and all constituent coils has been compared with calculated values obtained using field profile calculations and short sample J_c data. Good agreement between calculation and experiment has been found which shows that the top and bottom pancakes limit the performance of the magnet. The performance of the magnet is reduced by $\sim$20% due to the strain on the superconductor produced during the R + W technique. We conclude that a reliable fabrication technique has been described for the non-specialist to produce a R + W high-temperature superconducting laboratory-scale magnet.

Acknowledgments

The authors wish to thank H Jones and P Richens in the Magnet Group at Oxford University for their help and advice on coil winding, R Prowse for technical support winding the magnets at BICC General, G Teasdale and P Armstrong for fabrication of the magnet component parts, and P Russell and V Greener in help producing figures 4 and 5. This work was supported by EPSRC and BICC General.

References

[1] Bednorz J and Muller K 1986 *Z. Phys.* B **64** 189–93
[2] Wu M, Ashburn J, Torng C, Hor P, Meng R, Gao L, Huang Z, Wang Y and Chu C 1987 *Phys. Rev. Lett.* **58** 908–10
[3] Li Q, Brodersen K, Hjuler H and Freltoft T 1993 *Physica* C **217** 360–6
[4] Malozemoff A *et al* 1999 *IEEE Trans. Appl. Supercond.* **9** 2469–74
[5] Balachandran U, Iyer A, Jammy R, Chudzik M, Lelovic M, Krishnaraj P, Eror N and Haldar P 1997 *IEEE Trans. Appl. Supercond.* **7** 2207–10
[6] Zeng R, Lui H, Beales T and Dou S 1999 *IEEE Trans. Appl. Supercond.* **9** 2605–8
[7] Ohkura K, Sato K, Ueyama M, Fujikami J and Iwasa Y 1995 *Appl. Phys. Lett.* **67** 1923–5
[8] Kaneko T, Hikata T U M, Mikumo A, Ayai N, Kobayashi S, Saga N, Hayashi K, Ohmatsu K and Sato K 1999 *IEEE Trans. Appl. Supercond.* **9** 2465–8
[9] Leghissa M, Fischer B, Roas B, Jenovelis A, Wiezoreck J, Kautz S, Neumuller H, Reimann C, Nanke R and Muller P 1997 *IEEE Trans. Appl. Supercond.* **7** 355–8
[10] Larbalestier D and Lee P 1999 *Proc. 1999 Particle Accelerator Conf.* pp 177–81
[11] Sneary A, Friend C, Vallier J and Hampshire D 1999 *IEEE Trans. Appl. Supercond.* **9** 2585–8
[12] Sato K, Hikata T and Iwasa Y 1990 *Appl. Phys. Lett.* **57** 1928–9
[13] Snitchler G, Kaksi S, Manlief M, Schwall R, Sid-Yekhlef A, Ige S, Medeiros R, Francavilla T and Gubser D 1999 *IEEE Trans. Appl. Supercond.* **9** 553–8
[14] Sato K, Kato T, Ohkura K, Kobayashi S, Fujino K, Ohmatsu K and Hayashi K 2000 *Supercond. Sci. Technol.* **13** 18–22
[15] Zeng R, Zhou Y, Hua P, Fu X, Ye B, Zhou M, Yuan G, Lui H and Dou S 1998 *Supercond. Sci. Technol.* **11** 535–9
[16] Kumakura H, Kitaguchi H, Togano K, Wada H, Ohkura K, Ueyama M, Hayashi K and Sato K 1998 *Cryogenics* **38** 639–43
[17] Verges P, Fischer K, Hutten A and Fuchs G 1998 *Cryogenics* **38** 607–11
[18] Tomita N, Arai M, Yanagisawa E, Morimoto T, Kitaguchi H, Kumakura H, Togano K and Nomura K 1996 *Cryogenics* **36** 485–90
[19] Kerley N 1998 *Handbook of Applied Superconductivity; Vol. 2* ed B Seeber (Bristol: IOP Publishing) pp 1067–89
[20] Rabara M, Takeuchi T and Miya K 1999 *Physica* C **313** 213–18
[21] Oota A and Tanaka M 1996 *Physica* C **268** 295–9
[22] Fuller-Mora W 1996 *Phys. Rev.* B **54** 11 977–80
[23] Han G, Han H, Wang Z, Wang S, Wang F, Yuan W and Chen J 1994 *Cryogenics* **34** 613–16
[24] Hensel B, Grivel J, Jeremie A, Lerin A, Pollini A and Flukiger R 1993 *Physica* C **205** 329–37
[25] Hu Q, Weber H, Lui H, Dou S and Neumuller H 1995 *Physica* C **252** 211–20
[26] Kovak P, Husek I, Rosova A and Pachla W 1999 *Physica* C **312** 179–90
[27] Ekin J, Finnemore D, Li Q, Tenbrink J and Carter W 1992 *Appl. Phys. Lett.* **61** 858–60
[28] Polak M, Parrell J, Polyanskii A, Pashitski A and Larbalestier D 1997 *Appl. Phys. Lett.* **70** 1034–6
[29] Suenga M, Fukumoto Y, Haldar P, Thurston T and Wildgruber U 1995 *Appl. Phys. Lett.* **67** 3025–7
[30] Huang Y, ten Haken B and ten Kate H 1999 *IEEE Trans. Appl. Supercond.* **9** 2702–5
[31] Kovac P, Cesnak L, Melisek T, Husek I, Bukva P, Pitel J, Kopera L, Pachla W and Bucholtz W 1999 *Supercond. Sci. Technol.* **12** 507–13

[32] Vo N 1998 *J. Magn. Magn. Mater.* **188** 145–52
[33] Newson M, Ryan D, Wilson M and Jones H 2000 *IEEE Trans. Appl. Supercond.* **10** 468–71
[34] Hellstrom E 1995 *High-temperature Superconducting Materials Science and Engineering* ed D Shi (New York: Elsevier) pp 383–440
[35] Dou S and Liu H 1993 *Supercond. Sci. Technol.* **6** 297–314
[36] Flukiger R, Graf T, Decroux M, Groth C and Yamada Y 1991 *IEEE Trans. Appl. Supercond.* **27** 1258–63
[37] Grasso G, Jeremie A and Flukiger R 1995 *Supercond. Sci. Technol.* **8** 827–32
[38] Marti F, Grasso G, Grivel J-C and Flukiger R 1998 *Supercond. Sci. Technol.* **11** 485–95
[39] Zeng R, Beales T, Lui H and Dou S 1998 *Supercond. Sci. Technol.* **11** 299–303
[40] Han Z, Skov-Hansen P and Freltoft T 1997 *Supercond. Sci. Technol.* **10** 371–87
[41] Vo N, Willis J, Peterson D, Liu H and Dou S 1998 *Physica* C **299** 315–26
[42] Picard J *et al* 1999 *IEEE Trans. Appl. Supercond.* **9** 535–40
[43] Yang M, Goringe M, Grovenor C, Jenkins R and Jones H 1994 *Supercond. Sci. Technol.* **7** 378–88
[44] Ohmatsu K, Hahakura S, Kato T, Fujino T, Ohkura K and Sato K 1999 *IEEE Trans. Appl. Supercond.* **9** 924–7
[45] Tupper M, Fabian P and Beavers F 2000 *IEEE Trans. Appl. Supercond.* **10** 1350–3
[46] Wilson M 1998 *Superconducting Magnets* (New York: Oxford University Press)
[47] Celic E, Mutlu I, Avci E and Hascicek Y 2000 *IEEE Trans. Appl. Supercond.* **10** 1329–32
[48] Celic E, Mutlu I and Hascicek Y 2000 *IEEE Trans. Appl. Supercond.* **10** 1341–4
[49] Collings E 1986 *Applied Superconductivity, Metallurgy and Physics of Titanium Alloys* vol 2 (New York: Plenum)
[50] Evans D and Morgan J 1986 *Cryogenic Engineering* ed B Hands (London: Academic) pp 271–92
[51] Lee H and Neville K 1982 *Handbook of Epoxy Resins* (New York: McGraw-Hill)
[52] Baldan C, Shigue C and Filho E 2000 *IEEE Trans. Appl. Supercond.* **10** 1347–9
[53] Jones H and Hickman A 2000 *IEEE Trans. Appl. Supercond.* **10** 1345–6
[54] Brennan A, Miller T, Arnold J, Huang K, Gephart N and Markewicz W 1995 *Cryogenics* **35** 783–5
[55] Hands B 1986 *Cryogenic Engineering* ed B Hands (London: Academic) pp 241–70
[56] Sakuraba J, Mikami Y, Watazawa K, Watanabe K and Awaji S 2000 *Supercond. Sci. Technol.* **13** 12–17
[57] Kitaguchi H, Kumakura H, Togano K, Okada M, Tanaka K and Sato J 1998 *Cryogenics* **38** 181–6
[58] Jones H, Van Cleemput M, Hickman A, Ryan D and Saleh P 1998 *Physica* B **246–247** 337–40
[59] Keys S and Hampshire D 2001 *Handbook of Applied Superconductivity* (Bristol: IOP Publishing) to be published
[60] Herrmann P 1998 *Handbook of Applied Superconductivity; Vol. 1* ed B Seeber (Bristol: IOP Publishing) pp 801–43
[61] Meb K 1998 *Handbook of Applied Superconductivity; Vol. 1* ed B Seeber (Bristol: IOP Publishing) pp 527–55
[62] Selvaggi J, Mathewson W, Laughman R, Francavilla T, Gubser D and Miller M 1996 *Cryogenics* **36** 555–8
[63] Fabbricatore P, Priano C, Testa M, Musenich R, Kovac P, Martone A, Petrillo E and Ariante M 1998 *Supercond. Sci. Technol.* **11** 304–10
[64] Pitel J and Kovac P 1997 *Supercond. Sci. Technol.* **10** 847–52
[65] Sneary A, Friend C, Richens P, Jones H and Hampshire D 1999 *IEEE Trans. Appl. Supercond.* **9** 936–9
[66] Daumling M and Flukiger R 1995 *Cryogenics* **35** 867–70
[67] Montgomery D 1969 *Solenoid Magnet Design* (New York: Wiley)
[68] Tschopp W and Laukien D 1998 *Handbook of Applied Superconductivity; Vol 2* ed B Seeber (London: IOP) p 1191–212
[69] Hamid H and Hampshire D 1998 *Cryogenics* **38** 1007–15
[70] Gerhold J 1998 *Handbook of Applied Superconductivity; Vol. 1* ed B Seeber (Bristol: IOP Publishing) pp 1121–37